

## THE ZEEMAN EFFECT IN THE ANGSTROM CO BANDS

By E. C. KEMBLE,\* R. S. MULLIKEN, AND F. H. CRAWFORD

## ABSTRACT

**Theory of the Zeeman effect in the band lines of rigid diatomic molecules.**—The qualitative features of the Zeeman effect in the band lines of rigid diatomic molecules as given by the conventional quantum theory and the new quantum mechanics are the same. Both predict that the Zeeman pattern for electronic transitions of the type  ${}^1S \rightarrow {}^1P$  will be greatest for the first line in each branch (for which  $M$ , the empirical serial number of a line in a branch, is 1) and will increase in complexity ( $N$ =number of component lines in a pattern= $2M+1$ ) and decrease in scale as  $M$  increases. The size of the pattern is  $2/(M+1+1/4M) \cdot \Delta\nu_n$  on the old and  $2/(M+1) \cdot \Delta\nu_n$  on the new quantum theory. For  $M > 2$  the size of the pattern is almost exactly the same for both theories.

**Measurement of the Zeeman effect in the  $\lambda\lambda 5610, 5198$  and  $4835$  bands of CO.**—Results on the  $\lambda\lambda 5610, 5198$  and  $4835$  bands of CO are in agreement with the theoretical predictions. The effect is proportional to the field strength and the patterns are symmetrical about the positions of the lines with no field. Eight of the possible twelve patterns observable for the first two lines of the  $P$  and  $Q$  branches have been resolved, the rest together with all of the patterns for  $R(1)$  and  $R(2)$  being too faint for observation. With both polarizations superposed  $P(1)$  and  $Q(1)$  give symmetrical triplets of total width of 95 percent of  $\Delta\nu_n$ , thus falling almost exactly midway between the predictions of the two theories. The lines with  $M > 2$  are only partially resolved but give patterns which are characteristic and are in agreement with intensity predictions based both on the summation rule and the correspondence principle and on the quantum mechanics. The higher  $Q$  lines appear as doublets in the parallel polarization, and broad singlets in the perpendicular polarization. The  $P$  and  $R$  branches in the two polarizations show a similar, but reversed and less pronounced difference in character. A fact not accounted for by theory is the slightly greater intensity of the low-frequency components of the  $Q$  doublets (parallel polarization) and of the high-frequency components of the  $P$  doublets (perpendicular polarization). The results completely confirm the assignment by R. S. Mulliken of the CO Angstrom bands to electronic transitions of the type  ${}^1S \rightarrow {}^1P$  with  $\sigma' = 0$  and  $\sigma'' = 1$ , where  $\sigma$  is the electronic angular momentum parallel to the nuclear axis and single and double primes refer respectively to the initial and final states.

## INTRODUCTION

UNTIL quite recently there has been no satisfactory interpretation of the magnetic behavior of band spectra and the study of the Zeeman effect has played no part in the analysis of molecular spectra comparable with that which it has taken in connection with the study of atomic spectra. The primary reason for the backward condition of this phase of molecular spectroscopy is experimental, for the difficulties involved in the accumulation of empirical data are very great. The confusing nature of most of the observations made to date and the tardy growth of a satisfactory theory of the other characteristics of band spectra have also had much to do with

\* Fellow of the John Simon Guggenheim Memorial Foundation, 1927.

the slow development of an understanding of the Zeeman effect for bands. Recent theoretical advances, however, throw much light on the scattered empirical information gathered up to the present time and should be of great assistance to experimental workers in this field.

The experimental work described in this paper, which had its inception in the theoretical investigations of one of the authors,<sup>1,2</sup> leads to a much closer correlation of theory and experimental data than any published hitherto in this field. Hence we precede the description of our experimental technique and results by a brief review of the theoretical background of the problem.

#### SUMMARY OF THEORY<sup>2a</sup>

The first important theoretical contribution to the understanding of the magnetic behavior of band spectra was a brief discussion by Kramers and Pauli<sup>3</sup> of the application of the conventional Bohr theory to the problem of the Zeeman effect for a diatomic molecular model with an electronic angular momentum fixed in magnitude and rigidly oriented with respect to the nuclear axis. The same problem has been discussed somewhat more fully by Kemble<sup>1,2</sup> who independently reached essentially the same result. The formula given by Kramers and Pauli (in a somewhat altered notation) is

$$\Delta F = - (rH\mu/j^2) [(j^2 - \sigma^2)^{1/2} \sin \beta + \sigma \cos \beta] \quad (1)$$

Here  $\Delta F$  is the displacement of the "term" value  $F$  by the magnetic field  $H$ ,  $r$  is the magnetic quantum number, and  $j$  is the rotational quantum number which measures the total angular momentum of the molecule.  $\mu$  is the magnetic moment and  $\beta$  is the angle which it makes with the internuclear axis.  $\sigma$  is the component of the electronic angular momentum parallel to the nuclear axis in units of  $h/2\pi$ .

Hund,<sup>4</sup> in a notable paper on the theory of band spectra and its relation to the spinning electron hypothesis, has given theoretical reasons for supposing that normally the mean electronic angular momentum and the magnetic moment are parallel to the nuclear axis when the nuclear angular velocity is not too great, except in  $S$  states (where the mean orbital electronic angular momentum is zero). This conclusion is in harmony with Mulliken's scheme for the systematic interpretation of band spectra.<sup>5,6</sup> Aside from the  $S$  states, we may therefore set  $\beta$  equal to zero in equation (1). In view of the anomalous ratio of magnetic moment to angular momentum for the electron spin, the expression for  $\mu$  in terms of the corresponding quantum numbers is

$$\mu = (\sigma_k + 2\sigma_s)\mu_1 = (\sigma + \sigma_s)\mu_1 \quad (2)$$

<sup>1</sup> E. C. Kemble, Phys. Rev. **27**, 799A (1926).

<sup>2</sup> E. C. Kemble, Chapter VII, Section 6, of Bulletin 57 of the National Research Council, "Molecular Spectra in Gases."

<sup>2a</sup> For a more detailed account of the general theory, together with a review of the experimental literature, see reference (2).

<sup>3</sup> H. A. Kramers and W. Pauli, Jr., Zeits. f. Physik **13**, 351 (1923).

<sup>4</sup> F. Hund, Zeits. f. Physik **36**, 657 (1926).

<sup>5</sup> R. S. Mulliken, Proc. Nat. Acad. Sci. **12**, 151 (1926); ZnH, CdH, HgH bands.

<sup>6</sup> R. S. Mulliken, Phys. Rev. **28**, 481, 1202 (1926).

where  $\mu_1$  is the magnetic moment of the Bohr magneton and  $\sigma_k$  and  $\sigma_s$  are quantum numbers giving the respective contributions of the orbital motion and the spin to  $\sigma$ . Eq. (1) then takes the form

$$\Delta F = - [r(\sigma + \sigma_s)\sigma\mu_1 H] / j^2 \quad (3)$$

given by Hund. Eq. (3) is based on the assumption that the angular momentum of the electron spin  $s$  with respect to the nuclear axis is not appreciably disturbed by the nuclear rotation. Its applicability is therefore limited to singlet states for which  $s$  vanishes or, in the case of multiple electronic energy levels, to rotational states in which the product  $Bj$  ( $B = h/8\pi^2 I$ ) which measures the frequency of rotation is small compared with the spacing of the levels which form the multiplet. Hund also gives another Zeeman effect formula for use with large values of the ratio of  $Bj$  to the spacing of the levels in the multiplet, but this second case is not the one to which our data apply.

Van Vleck<sup>7</sup> has recently called attention to the fact that a possible modification of (3) in conformity with the new quantum mechanics is implicitly contained in a paper by Dennison<sup>8</sup> on the application of the quantum mechanics to the symmetric rigid rotator. Van Vleck gives the explicit formula

$$\Delta F = - \frac{r\mu\sigma H}{j^2 - \frac{1}{4}} = - \frac{r(\sigma + \sigma_s)\sigma\mu_1 H}{j^2 - \frac{1}{4}} \quad (4)$$

which differs from (3) only in the substitution of  $j^2 - 1/4$  for  $j^2$ . The formula assumes that the conventional empirical values of  $j$  ( $j = \sigma + 1/2, \sigma + 3/2, \dots$ ) are to be used. If these values are all reduced by  $1/2$  in accordance with the usual notation of the quantum mechanics, the denominator in Eq. (4) becomes  $j(j+1)$ . We shall adhere to the usual band spectrum convention regarding  $j$  in this paper, however,—thereby fixing the maximum and minimum values of the magnetic quantum number  $r$  consistent with any given  $j$  as  $j - 1/2$  and  $-(j - 1/2)$  respectively. Hence in this notation the number of magnetic sub-levels associated with any given rotational state, i.e., its a priori probability, is  $2j$ .

These theories all agree qualitatively. For example, all of them require that the scale of the Zeeman pattern shall be greatest for the faint lines adjacent to the origin and shall diminish rapidly as the rotational quantum number  $j$  increases, so that the outer lines of a band should be magnetically insensitive. They also require that each parent energy level shall be resolved by a magnetic field into equally spaced sublevels, the number of which is exactly or approximately equal to  $2j$ . Hence the complexity of the Zeeman pattern should increase as its scale decreases. Since the theories are all based on the assumption that the molecule executes a uniform precession in the magnetic field, the principle of selection  $r' - r'' = 0, \pm 1$  is equally applicable in all three cases.

<sup>7</sup> J. H. Van Vleck, Phys. Rev. **28**, 980 (1926).

<sup>8</sup> D. M. Dennison, Phys. Rev. **28**, 318 (1926).

In the light of the above theories and of the systematic interpretation of band spectra made possible by the recent work of Mulliken<sup>5,6,9,10</sup> and Hund,<sup>4</sup> the complete absence of a first order Zeeman effect (i.e. of a magnetic resolution of the lines into components having displacements of the same order of magnitude as for line spectra) is to be expected in the case of certain band types. Thus electronic states of the  $^1S$  type have no normal magnetic moment<sup>10a</sup> and bands of the  $^1S \rightarrow ^1S$  type should accordingly show no first order Zeeman effect. Moreover, in the case of  $^2S$  and  $^3S$  states the normal magnetic moment is associated solely with the electron spin and is coupled to the molecular axis by very weak forces which vanish with the nuclear rotation. Hence even a small magnetic field should effectively break this loose coupling and create a Paschen-Back effect in which the molecule behaves as if the spin magnetic moment did not exist. Thus we may generalize the above statement regarding bands of the  $^1S \rightarrow ^1S$  type and say that no first order Zeeman effect is to be expected from any  $S \rightarrow S$  transitions.

Hitherto the experimental work on the Zeeman effect for bands has been fragmentary in character and not well adapted to testing even the fundamental qualitative requirements of the theory. A general review of the experimental literature is given in reference 2. The experimental situation may be summarized briefly as follows: (a) most bands are much less sensitive to magnetic influence than line spectra; (b) the lines near the origin are as a rule more sensitive than the lines farther from the origin, and frequently show first order Zeeman patterns comparable in scale with the patterns of typical atomic lines; (c) no first order Zeeman effect has been observed in the case of  $S \rightarrow S$  bands; (d) the bands most studied, such as the  $\lambda 3900$  CH band,<sup>11,12</sup> show a variety of anomalous effects indicating that the molecule is distorted by the field so that the rigid molecule theories are not applicable. Thus the existing data are on the whole in qualitative agreement with the requirements of theory, but fail to confirm it with any degree of completeness. With respect to the important predicted increase in the complexity of the Zeeman pattern with increasing rotational quantum number, no conclusive evidence has been found, and it was primarily in the

<sup>9</sup> R. S. Mulliken, Phys. Rev. **29**, 391 (1927); intensity relations.

<sup>10</sup> R. S. Mulliken, Phys. Rev. **29**, May (1927); Hund's theory, etc.

<sup>10a</sup> By a "normal magnetic moment" we mean a magnetic moment characteristic of a non-rotating molecule. Evidence has been given by Knauer and Stern [Zeits. f. Phys. **39**, 780 (1926)] and by one of the present writers (reference 2, page 345) indicating that a small magnetic moment in the direction of the  $j$  axis is produced either directly or indirectly by the rotation of the nuclei. The rotational magnetization may produce a second order Zeeman effect for the outer lines in a band even when the "normal magnetic moment" is zero for both of the associated electronic states. This second order effect will not be taken into consideration in this paper, however.

<sup>11</sup> E. Hulthén, Thesis, Lund, (1923).

<sup>12</sup> R. Fortrat, Ann. de Physique **19**, 81 (1923). This paper purports to be a study of the Zeeman effect in the  $\lambda 3872$  Swan band, but R. T. Birge has kindly called our attention to the fact that the wave-lengths given by Fortrat prove that the band which he studied was really the  $\lambda 3900$  CH band.

hope of securing definite confirmation of this theoretical prediction that the present investigation was undertaken.

In order to test theories based on the assumption that the magnetic moment is rigidly oriented with respect to the nuclear axis one must, of course, pick out bands for which this assumption is approximately fulfilled. Now, as Hund has pointed out, there is reason to believe that the angular momentum and magnetic moment originating in the orbital motion of the electrons is quite rigidly bound to the nuclear axis, while the angular momentum due to electron spin is loosely attached. Hence the most rigid molecular states should be those in which the spin vector vanishes, i.e., those of the singlet system. We have therefore chosen the Angstrom CO, bands which are of the  ${}^1S \rightarrow {}^1P$  type<sup>6</sup> and lie in a favorable part of the spectrum. These bands have a very simple structure with singlet *P*, *Q*, and *R* branches. The rotational term formula

$$F(j) = B(j^2 - \sigma^2) \quad j = -1/2, 3/2, 5/2; \quad (5)$$

fits the data very well if  $\sigma$  is given the values 0 and 1 for the upper and lower electronic levels respectively. This fact affords direct evidence of the rigid character of the initial and final states.

Since  $\sigma$  vanishes for the upper energy level and the angular momentum of spin is also zero, the upper level can have no magnetic moment and should contribute nothing to the Zeeman pattern. Denoting the lower energy level by a double prime and setting  $\sigma'' = 1$ ,  $\sigma_s'' = 0$ , we may write out the following special forms of equations (3) and (4) applicable to the Angstrom CO bands:

$$\Delta F = r'' \mu_1 H / j''^2 \quad (3A); \quad \Delta F = r'' \mu_1 H / j''^2 - \frac{1}{4} \quad (4A)$$

These formulas become definite only when the values to be assumed by  $r''$  are specified. The new quantum mechanics on which Eq. (4A) is based requires that  $r''$  shall take on the values  $\pm(j'' - 1/2)$ ,  $\pm(j'' - 3/2)$ , etc. Independently of the new mechanics we arrive at the same result by observing that in the case of atoms the a priori probability of any parent state is  $2r_{\max} + 1$  whether the number of electrons be odd or even. Moreover, in the case of diatomic molecules the a priori probability is always  $2j$  as required by the summation rule and confirmed by the quantitative intensity measurements of Bourgin and Kemble<sup>13</sup> for HCl, as well as by other work on even<sup>9</sup> and odd<sup>14</sup> molecules. Hence  $2r_{\max} + 1$  is equal to  $2j$  or  $r_{\max} = (j - 1/2)$ .

We can now predict the exact character of the magnetic structure of each of the rotational levels associated with the lower electronic state. The minimum value of  $j''$  is  $3/2$  (equal to  $\sigma'' + 1/2$ ). Hence the lowest rotational state should split into three magnetic sub-states corresponding to values 0, +1, -1 of the magnetic quantum number  $r''$ . The spacing

<sup>13</sup> E. C. Kemble and D. Bourgin, *Nature*, June 5, (1926). D. Bourgin, *Phys. Rev.* **29**, 794 (1927).

<sup>14</sup> R. S. Mulliken, F. A. Jenkins, and H. A. Barton, *Nature* **119**, 118 (1927); *Phys. Rev.* **29**, 211A (1927) and later articles: NO bands.

of the components of this triplet should be  $4/9$  of the "normal" spacing,  $\mu_1 H$ , according to Eq. (3A) and  $1/2$  "normal" according to Eq. (4A). The second rotational level should yield five components with a spacing  $4/25$  normal or  $1/6$  normal according to Eqs. (3A) and (4A) respectively. The magnetic structures of these two rotational energy levels should be reproduced in the Zeeman patterns of the first and second lines, respectively, of each of the three branches.

If we denote the ordinal number of any line in the corresponding branch by  $M^{14a}$  and set  $M$  equal to unity for the first observed line of each branch, we have  $M = j'' - 1/2$  and the general rule for the number of Zeeman components  $N$  in the pattern of any given line is

$$N = 2j'' = 2M + 1$$

The over-all width of the Zeeman pattern for the  $M$ th line is

$$\Delta\nu = \frac{\mu_1 H(2j'' - 1)}{j''^2} = \frac{2M\mu_1 H}{(M + \frac{1}{2})^2} = \frac{2\mu_1 H}{M + 1 + \frac{1}{4}M} = \frac{2\Delta\nu_n}{M + 1 + \frac{1}{4}M} \quad (6)$$

according to Eq. (3A), and

$$\Delta\nu = \frac{2\mu_1 H}{M + 1} = \frac{2\Delta\nu_n}{M + 1} \quad (7)$$

according to Eq. (4A).

In order to predict the appearance of the Zeeman patterns as observed with a spectroscope with insufficient power to resolve completely the fine structure, it is necessary to compute the intensities of the components. For this purpose we may use the intensity formulas deduced for line spectra by Kronig and by Hönl from the summation rule.<sup>15</sup> The applicability of these formulas to bands has the same justification as for line spectra. In order to show the relative intensities of components belonging to different parent lines, the Zeeman intensity formulas may be combined with the Hönl and London formulas for the intensities of the unperturbed band lines.<sup>16</sup> The combination formulas are in harmony with those deduced from the matrix mechanics by Dennison<sup>8</sup> for the Zeeman components of the spectrum lines of a rigid symmetrical rotator. When  $\sigma'$  and  $\sigma''$  are given the values 0 and 1 respectively the equations take the form:

$$P \text{ branch } \begin{cases} I_0 = \frac{3(M^2 - r''^2)(M + 1)}{(2M - 1)(2M + 1)M} \\ I_{\pm 1} = \frac{3(M \pm r'')(M \pm r'' - 1)(M + 1)}{4M(2M - 1)(2M + 1)} \end{cases} \quad (8A)$$

<sup>14a</sup> i. e.  $M$  is equal to the value of  $j''$  as used in the new quantum mechanics.

<sup>15</sup> R. de L. Kronig, *Zeits. f. Physik* **31**, 885 (1925); H. Hönl, *Zeits. f. Physik* **31**, 340 (1925).

<sup>16</sup> H. Hönl and F. London, *Naturwiss.* **13**, 756 (1925); *Zeits. f. Physik* **33**, 803 (1925).

$$Q \text{ branch} \begin{cases} I_0 = \frac{3r''^2}{M(M+1)} & (9A) \\ I_{\pm 1} = \frac{3(M \pm r'')(M \pm r'' + 1)}{4M(M+1)} & (9B) \end{cases}$$

$$R \text{ branch} \begin{cases} I_0 = \frac{3[(M+1)^2 - r''^2]M}{(M+1)(2M+1)(2M+3)} & (10A) \\ I_{\pm 1} = \frac{3(M \mp r'' + 1)(M \mp r'' + 2)M}{4(M+1)(2M+1)(2M+3)} & (10B) \end{cases}$$

Here  $I_0$ ,  $I_{+1}$ , and  $I_{-1}$  are the intensities of the components associated with the transitions  $r'' = r' + 0$ ,  $r'' = r' + 1$ ,  $r'' = r' - 1$ , respectively, for transverse observation. As the components  $I_{+1}$  and  $I_{-1}$  for any given value of  $r''$  are superimposed, in the present case, because of the lack of Zeeman splitting

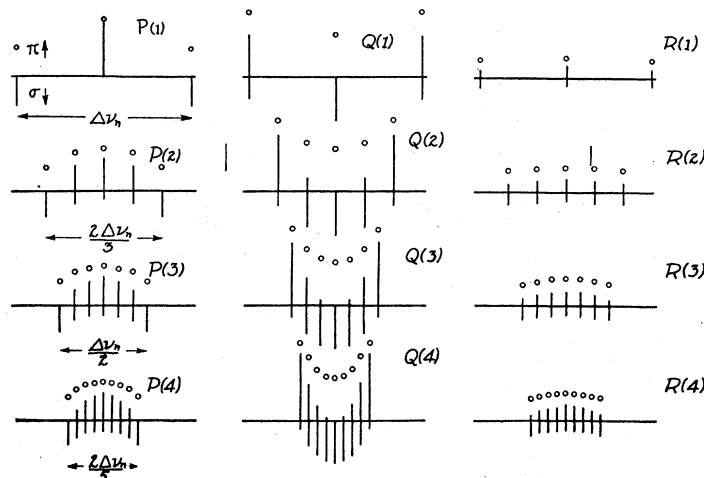


Fig. 1. Theoretical Zeeman patterns for  $P$ ,  $Q$ ,  $R$  lines of  $1S \rightarrow 1P$  bands. The magnitudes of the patterns are calculated from Eq. (4A) and the intensities from Eqs. (8A) to (10B) inclusive. (These equations take account of the relative intensity of the lines in a band.) Intensities calculated for the case of polarization ( $\pi$ ) parallel to the field are plotted upward from the horizontal lines, while those plotted downward are for polarization perpendicular ( $\sigma$ ) to the field. The intensities with both polarizations superposed are represented by the small circles. The distance between outermost components for a given value of  $M$  is the same in each branch.

in the initial electronic state, their intensities must be added to get the total intensity of the corresponding line with polarization perpendicular to the lines of force.

Figure 1 shows the positions and relative intensities of the Zeeman components of the first four lines of each branch as computed from Eqs. (4A), (8A), (8B), (9A), (9B), (10A), (10B) for transverse observation with both polarizations. The parallel or  $\pi$ -components ( $I_0$ ) are plotted above the zero

line and the perpendicular or  $\sigma$ -components ( $I_{+1}$ ,  $I_{-1}$ ) below the zero line. It will be apparent at once that the early lines in the  $Q$  branch as observed in a spectroscope with moderate resolving power (insufficient to give the full structural detail) should appear to be doublets in the parallel polarization and (with the exception of  $Q(1)$ ) broad singlets in the perpendicular polarization. The two polarizations of the  $P$  and  $R$  branch lines should show a similar, but reversed and less pronounced difference in character.

#### APPARATUS AND EXPERIMENTAL DETAILS

The light source was an uncondensed high-potential alternating discharge passing between copper electrodes in an atmosphere of  $\text{CO}_2$ . The gas was contained in a Back-box<sup>17</sup> enclosing the magnet poles of a large Weiss-electromagnet. The pole-tips of this magnet were about 7 mm in diameter and when kept about 5 mm apart gave a maximum field of around 35,000 gauss. The discharge passed parallel to the field between disc or wiring electrodes, the light from the discharge being sent through a quartz window and lens and focussed on the slit of a 21-foot concave grating. This was arranged in the Paschen mounting,<sup>18</sup> so that the entire spectrum could be photographed at once.

The  $\text{CO}_2$  was generated by the action of pure  $\text{HCl}$  on marble, being then passed in succession through  $\text{NaHCO}_3$  solution and granulated  $\text{CaCl}_2$  to remove  $\text{HCl}$  and moisture. During the runs, a slow stream of  $\text{CO}_2$  was pumped through the Back-box, in order to minimize the effect of impurities due to possible leakage and to the liberation of gases by the action of the discharge. Best results were obtained when the  $\text{CO}_2$  pressure was maintained at 8 mm or less.

The magnet is one of the standard Weiss types with water-cooled copper coils and can be operated on a current between 60 and 70 amperes indefinitely without serious heating. Since with currents of this magnitude the iron was nearly saturated, satisfactory constancy of field was obtained by regulating the field current to an ampere or less. The necessary current was supplied at about 60 volts by a 5-kw motor-generator set operating on a 550-volt line. Preliminary to a run, the field current was allowed to flow until approximately constant temperature conditions were established in the magnet.

*Design of Back-box.* The Back-box was built in the Laboratory shop essentially according to Back's description, but with certain modifications. In Back's design (l.c., p. 124) the ends of the box are separated from the pole pieces by means of rubber gaskets, and troublesome adjustments were necessary to keep the faces of the pole pieces parallel and thus to insure a uniform field despite the distortion of the magnet yoke at the higher fields. In order to avoid these adjustments and to keep the pole faces automatically parallel, the following changes were made. (See Fig. 2) Both pole pieces

<sup>17</sup> Cf. E. Back and A. Landé, *Zeemaneffekt und Multiplett Struktur der Spectrallinien*. Pp. 122-31, Julius Springer, Berlin (1925).

<sup>18</sup> Cf. E. Back and A. Landé, l.c., p. 150.



were cut off squarely from their stems and the back of one was given a convex-spherical shape (see Fig. 2 at *B*) in a lathe. The corresponding magnet-stem was then turned to fit the back of the pole piece. The two pole pieces (with shoulders cut to fit snugly) were finally inserted in the cylindrical box,

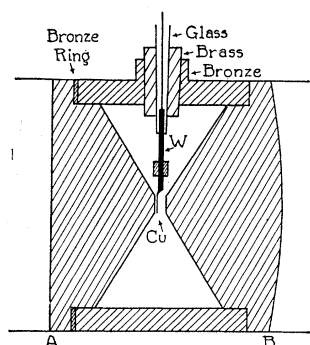


Fig. 2. Modified Back box.

the joints being made air-tight by rings of soft wax. To allow for varying gap lengths a series of bronze gaskets were provided which could be inserted between the shoulders of the pole pieces and the ends of the box. The rigid unit of pole pieces and box was then inserted in the magnet so as to complete the magnetic circuit. The spherical end enabled centering to take place almost automatically. By increasing the pressure on the box and pole pieces by means of the main adjusting screws of the magnet, (not shown in figure) most of the wax was extruded, the thin films remaining showing no discernible tendency to allow even slight buckling of the magnet frame. The box was provided with four windows, and with an inlet and an outlet tube at opposite sides. In addition to the electrodes for gas excitation, two electrodes were provided for obtaining an interrupted metal arc,<sup>17</sup> to provide standard lines for the determination of field strengths.

*Electrodes.* The discharge electrodes had tungsten leads in tapered pyrex plugs. The latter were ground to fit into brass plugs which were themselves conical and ground to fit into openings in the box. The ground joints were kept tight with stop-cock grease. By means of a small brass sleeve with set screws, the actual electrodes were fastened to the leads. The chief difficulties are the elimination of stray discharge between the electrode leads and to the pole pieces, and the keeping of the electrodes properly centered and at the optimum separation. Stray discharge is especially noticeable at low pressures. If the pressure is raised to lessen this stray discharge (or if a condensed discharge is used), undesired band spectra appear, as well as the line spectrum of the electrodes, while the CO Angstrom bands are weakened. (The total luminous intensity may at the same time be much increased.) The second negative carbon bands of Deslandres and D'Azambuja are regularly present, especially at higher pressures, but cause no serious trouble, since they are in the ultra-violet. The discharge has a greenish-blue color when the CO Angstrom bands are strong.

Various forms of electrodes were tried. A simple and good one can be made from a piece of No. 16 copper wire, by bending one end into a ring 5 mm in diameter, flattening slightly, and sheathing the stem with a piece of capillary pyrex or silica tubing. The pole pieces must also be insulated, e.g. by fitting glass caps over them (fastened with de Khotinsky cement) or using thin pieces of mica attached to the electrodes themselves. In operation such electrodes become red hot even with the minimum current

in the primary of the transformer, and consequently eventually burn away and must be replaced.

*Exposures.* Most of the exposures were made with a field of about 35,000 gauss. One exposure (no polarization) was made with about 24,000 gauss (for this a magnet current of 14 amperes was needed). In another (no polarization) a comparison was made of the spectrum with a field of 35,000 gauss and that with the residual field of the magnet, which served as "zero field." (Actually there was even here a very slight broadening of the lines of widest Zeeman pattern.) Most of the exposures were made with a Nicol prism interposed in front of the slit so as to give light polarized either parallel, or perpendicular, to the direction of the field.

Exposures up to forty-two hours were made, during which the electrodes had to be replaced occasionally. With the co-operation of Mr. R. A. Loring, a continuous plate-holder was arranged to keep the plates at the position of best focus, the latter having been carefully redetermined throughout the spectrum. Photographs were taken in the first and second orders, using Eastman Speedway plates (or in some cases Eastman 33) below 4900Å, and Eastman Astronomical Green Sensitive plates up to about 5900Å. After each exposure, the plates, and the gas electrodes, were removed without interrupting the magnet current; a photograph was then taken with the other electrodes so as to obtain the Zn triplet  $\lambda\lambda 4660, 4722, 4811$  for use as a field standard.<sup>19</sup> Or in some cases this was omitted and the Cu lines  $\lambda\lambda 3247, 3274$ , which were always present on the band plates (because of the use of Cu electrodes) were used as field standards. Photographically the most intense bands in the first order were the green bands  $\lambda 5610$  (0, 3) and  $\lambda 5198$  (0, 2), followed by  $\lambda 4835$  (0, 1),  $\lambda 4511$  (0, 0),  $\lambda 4123$  (1, 0), and  $\lambda 4394$  (1, 1); the numbers in parentheses are the vibrational quantum numbers.<sup>20</sup>

Six sets of plates, with exposures varying between 5 and 42 hours, gave the first four of these bands in sufficient intensity in the first order so that some of the lines in each of the above bands could be studied. The plates of the last two bands were rendered completely useless by the presence of an intense background of impurity lines. The band  $\lambda 4511$ , not having been thus far analyzed,<sup>21</sup> is reserved for future discussion, the present paper being confined therefore to the bands  $\lambda\lambda 5610, 5198$  and  $4835$ .

The chief difficulty, of course, lies in the fact that the lines which can be resolved into Zeeman patterns are those which correspond to the lowest values of  $j$  and which at ordinary temperatures, due to the fairly large moment of inertia of the CO molecule, are of *very* low intensity. The second order of the grating being considerably weaker (over the range of wave lengths

<sup>19</sup> The Zeeman separations for these lines have been shown to be accurately proportional to field strengths. See Cotton and Weiss, *Journal de physique* **6**, 429 (1907). The magnetic field was calculated from the expression  $H = \Delta\nu_n / 4.698 \times 10^5$  where  $\Delta\nu_n$  is the normal Lorentz separation in wave-numbers as obtained from the zinc lines.

<sup>20</sup> For assignment of vibrational quantum numbers see: R. T. Birge, *Phys. Rev.* **28**, 1157 (1926).

<sup>21</sup> O. Jasse, *Comptes rendus* **182**, 692 (1926).

used) than the first, the second order plates were of use only for certain strong  $Q$  lines somewhat removed from the band origins.

Plate measurements were made on a Max Wolz comparator on which 0.0001 cm could be estimated. The quantities to be measured varied in magnitude from 0.02 cm to about 0.005 cm, the extreme faintness of the earlier patterns and the lack of definition of the higher rendering the accuracy of a given reading in all cases much less than the graduations of the comparator would suggest. It was consequently necessary to average a great number of settings (as high as 20 or 30) made at various points along a given line. The dispersion at any point was obtained from measurements on unaffected lines using the frequency differences given by Hulthén.<sup>22</sup>

*Temperature control in grating room.* The natural variations in the temperature of the grating (which is in a basement room) were found to be too great to give the desired line-sharpness. Hence, during the exposures the temperature of the grating room was maintained constant to less than 0.1°C (probably to  $\pm 0.03^\circ$  or  $0.04^\circ\text{C}$ ) by thermostatic control. Heating

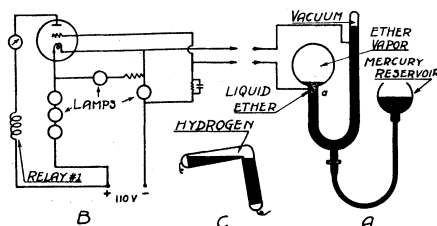


Fig. 3. When the ether vapor contracts sufficiently, an electrical contact is made at  $a$  which short-circuits the grid to the filament, thus changing the plate current and operating relay number 1. This actuates a second heavier relay which tips the mercury circuit breaker shown at  $C$  and turns on the current in the heating coils.

was accomplished by means of forty foot lengths of number 22 nichrome wire, connected in parallel and strung along one wall and so adjusted that each took a current of 5 amperes from a 110-volt line. Air circulation was provided by an electric fan on the other side of the room.

The details of the thermostatic control are given schematically in Fig. 3.  $A$  represents a temperature control device constructed with the co-operation of Dr. F. A. Jenkins. It may be set for any desired temperature by varying the height of the mercury reservoir, its operation being clear from the diagram. The advantages of this device are its reliability and its responsiveness. By using only very minute currents and having a layer of (liquid) ether over the mercury at  $a$  (the bulb is filled with air-free ether vapor) fouling of the mercury surface on make and break is almost completely prevented. Since, furthermore, ether has a large vapor pressure at room temperatures, small temperature differences cause a considerable displacement of the mercury levels with resultant high sensitivity. The avoidance, moreover, of sparking on break of circuit, by preventing the consequent heating, reduces the time lag in operation.

<sup>22</sup> E. Hulthén, Thesis, Lund (1923).

This control device was used to operate the vacuum tube relay shown in Fig. 2B. The latter is an adaptation of an idea described by H. S. Roberts<sup>23</sup> and is used to actuate a very small telephone relay (Relay 1). This then operates a larger telegraphic relay which in turn works the  $L$ -circuit-breaker shown at  $C$ . This circuit-breaker contains hydrogen under a pressure of several atmospheres over the mercury and is capable of breaking a current of 15 amperes or more without danger.

In practice the control device was adjusted for an amount (usually  $0.5^\circ$  to  $1.0^\circ$ ) sufficiently above the slowly changing room temperature to provide a safe operating margin. In the case of very long exposures where a greater margin of safety was necessary, an additional continuous heater, capable of producing an elevation of from  $0.5^\circ$  to  $1.0^\circ$ , was employed, its use being confined to the beginning or end according as the natural room temperature was slowly rising or falling

#### RESULTS

The effects produced by the magnetic field on the bands studied here are in general of two sorts, (1) those effects noticeable near the origin and covered by the theory given in this paper, and (2) certain perturbations found only in the higher lines (i.e.  $M=26$  to  $29$ ) and apparently confined chiefly to one line in each branch. These latter effects manifest themselves as more or less symmetrical patterns of total width several times the normal effect,  $\Delta\nu_n$ , together with a light continuous (or presumably unresolved) background. Due to uncertainty caused by the possible presence of impurity lines superposed on these patterns, their discussion is reserved until further data have been obtained.<sup>24</sup>

In comparing the experimental data with the theoretical predictions, it is well to remark at the outset that the displacements observed seemed always to be symmetrical around the undisplaced positions of the lines.<sup>25</sup> Furthermore, the data for the widths of the  $Q(1)$  pattern with fields of 24,400 and 34,900 gauss respectively showed that the size of the pattern was a linear function of the field (to within  $\pm 2$  per cent). In addition there remain three general heads under which theory and experiment can be compared, viz. occurrence or nonoccurrence of (1) predicted types of pattern in a given state of polarization, (2) proper relative intensity of components in individual patterns and in neighboring ones, and finally (3) correct quantitative scale of patterns. Since no microphotometric measurements have thus far been made, the first two tests are essentially qualitative. (See footnote 33).

<sup>23</sup> H. S. Roberts, Jour. Opt. Soc. Am. **11**, Aug. 1925.

<sup>24</sup> Because of the length of time required for exposures, an exposure with field was taken alongside one without on only one set of plates. This, however, served for the location of the faint impurity lines which might be expected to cause ambiguity in measuring the weaker Zeeman patterns. In the case of only one or two of the band lines discussed in the present paper did such impurities cause difficulty.

<sup>25</sup> Future plates taken with zero field comparison exposures may serve to reveal slight bodily shifting of patterns, although such effects must be very small if they exist.

Because of the varying arrangement of the lines in the three bands used, only rarely can the same line be studied in each band. Frequently a pattern partially obscured by another line or rendered ambiguous by an impurity for one field can be measured for a larger or smaller field. To render clear the cases in which difficulties of this sort occur, the earlier lines of the bands under consideration are given schematically in Fig. 4, the relative intensities

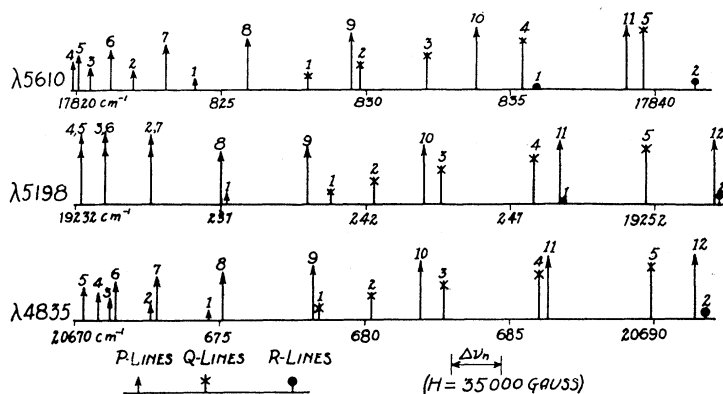


Fig. 4. Schematic diagrams showing the arrangement of the lines in the *P*, *Q* and *R* branches near the head of the three Angstrom CO bands considered in this paper. Ordinates represent relative intensities. Double arrowheads indicate superposition of two lines. To aid in following the text  $\Delta\nu_n$  for  $H = 35,000$  gauss is plotted to scale.

of the lines in the same band being indicated by the height of the corresponding ordinates.<sup>26</sup> For comparison the scale of the Zeeman pattern for  $H = 35,000$  gauss is represented by a line equal in length to  $\Delta\nu_n$ . When it is considered that only the first two lines of the *P* and *Q* branches were definitely resolved into their fine line patterns and that the pattern for either *P*(2) or *Q*(2) consists normally of four or five separate components, the difficulties regarding intensity are thrown sharply into relief.

*Notation.* The lines whose fine-structure could be studied will be considered singly and in some detail, the higher lines requiring little individual attention. In order to be able to refer to the individual components of a given line, we shall adopt a convenient notation, writing for example  $\pi - P(2)_{-2}$  to designate that component, in parallel polarization, of the *P* line for which  $j'' = 5/2$  (i.e. for which  $M = 2$ ) and  $r'' = -2$ ;  $\pi - \sigma - P(2)_{-2}$  to designate the same with both polarizations superposed, etc.<sup>27</sup>

*Structure of P(1).* Beginning with the *P* lines we find that in parallel polarization in both  $\lambda 5610$  and  $\lambda 4835$  *P*(1) occurs in the presence of the

<sup>26</sup> R. S. Mulliken, Phys. Rev. **29**, 411 (1927).

<sup>27</sup> Since there is no experimental means of determining the orientation of a given molecule in the magnetic field, the above notation regarding  $r''$  values is purely arbitrary. If it be assumed that components having a higher frequency than the undisplaced line result from transitions in which  $r''$  is negative, then those having a lower frequency result from transitions in which  $r''$  is positive.

field as a sharp singlet in the original position of the line (not favorably situated for observation in  $\lambda 5198$ , (of Fig. 4). Its intensity is about the same as that of  $\pi - Q(1)_{-1}$ , but distinctly greater than that of  $\pi - Q(1)_{+1}$ . (According to Fig. 1, of course, these two  $Q$  components should be of equal intensity; cf. below.) In the perpendicular polarization it occurs in  $\lambda 5198$  as a symmetrical doublet, whose components are displaced by equal and opposite amounts on either side of the zero-field position. Were an undisplaced component also present, it would of course be obscured by  $P(8)$ . That such is not present is shown by the fact that in  $\lambda 4835$  no line occurs at the undisplaced position (the displaced components are here not favorably situated for observation). When both polarizations are superposed we have a triplet ( $\lambda 5610$ ) with the central component much the more intense. It is about the intensity of  $\pi - \sigma - Q(1)_{+1}$ . Although this is the only plate showing the outer components of the  $P(1)$  pattern with sufficient intensity for comparison,<sup>28</sup> it is significant that the  $P(1)_{-1}$  component is much more intense than the  $P(1)_{+1}$ . This, if confirmed on future plates, is a fact not accounted for by the theory. It is to be correlated with the dissymmetry in the corresponding  $Q$  patterns in parallel polarization, the difference being that in the first case the component of *higher* frequency is the more intense, while in the latter the reverse is true.<sup>29</sup>

It is to be noted that in making the enlargements from which the reproductions in Fig. 5 were made the weak lines near the head had to be exposed about twice as long as the higher-numbered lines in order that they should be visible at all on the reproduction. Consequently, although the relative intensities of say the  $P(1)$  and  $Q(1)$  patterns are preserved, these patterns appear much more intense (when compared with the stronger  $P$  lines) in the figure than on the original plates.

For the numerical width of the  $P(1)$  triplet, Eq. (3A) predicts 88.9% and Eq. (4A) 100% of  $\Delta\nu_n$ . The observed widths are given in Table III, the value from  $\lambda 5610$  being much the more reliable. The observed values lie near the arithmetical average of the predictions of the two theories (cf also results for  $Q(1)$  lines).

<sup>28</sup> As Fig. 1 shows the outer lines of the  $P(1)$  pattern with both polarizations superposed should be of the same intensity as with perpendicular polarization alone. This follows from the fact that for parallel polarization where  $\Delta\nu=0$ , Eq. (8A) gives  $I_o=0$ . Consequently the outer components in this polarization have zero intensity. Hence when both polarizations are superposed, whatever intensity these outer components have is due to transitions for which  $\Delta r = \pm 1$ , i.e. is due solely to light polarized perpendicularly to the field.

<sup>29</sup> It should be pointed out that in all probability the final states for the  $P$  and  $R$  lines of these bands are not identical with those for the  $Q$  lines ( $\sigma$ -type doubling). The separation of these two final states (which we may refer to as  $A$  and  $B$  rotational substates; see R. S. Mulliken Phys. Rev. **28**, 1202 (1926), Fig. 1, also Phys. Rev. **29**, 637 (1927)) for the Angstrom bands is practically zero for low  $M$  values, but becomes large enough to be noticed for large  $M$  values. (See E. Hulthén, Thesis, where the resulting combination defect was first noted.) It is likely then that the difference in the intensity dissymmetry in the  $P$  and  $Q$  patterns is correlated with the difference in the final states of these lines (the initial states being magnetically insensitive). The dissymmetry itself is probably a function of the field strength disappearing for very low fields. This question will be considered in another paper.

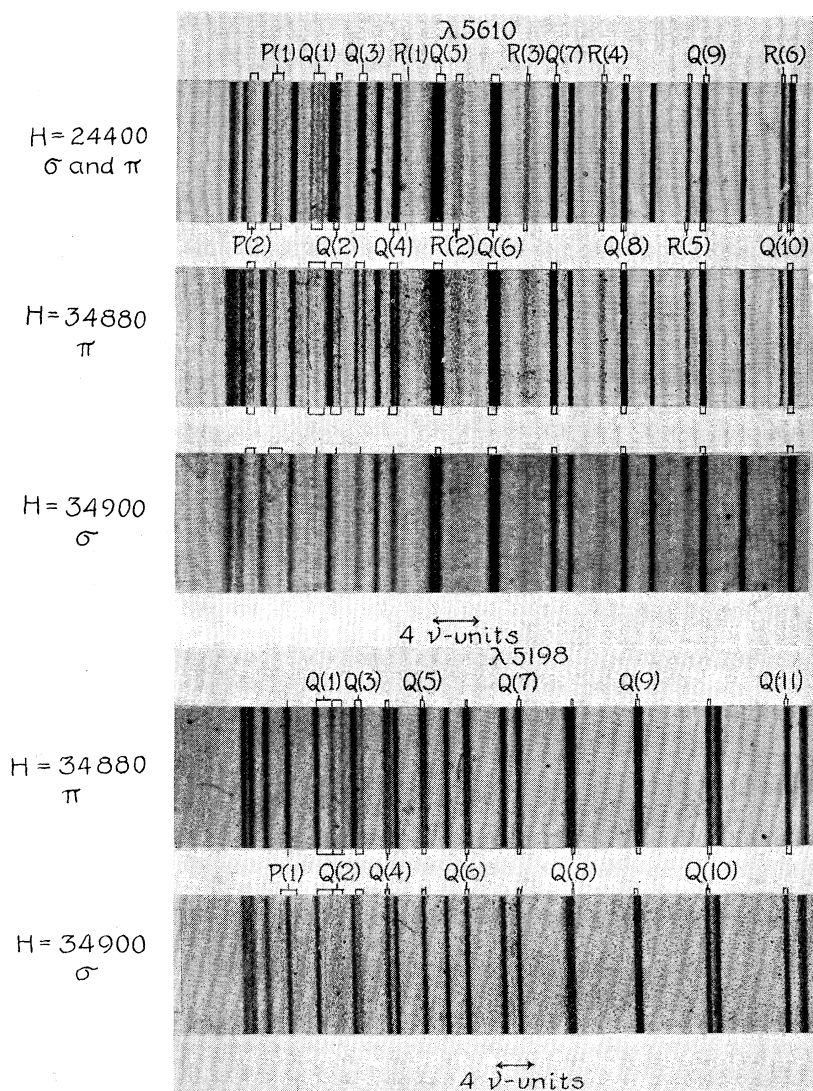


Fig. 5. These reproductions represent enlargements (about 15 times) of regions near the heads of the  $\lambda\lambda 5610$  and  $5198$  bands. In order to insure the reproduction of at least some of the fainter patterns the left ends of the bands (as explained in the text) were exposed longer in printing than the rest. Consequently the patterns of the  $P(1)$ ,  $P(2)$ ,  $Q(1)$ , and  $Q(2)$  lines have a much greater relative intensity than on the original plates. Faint lines not marked are impurities (including the faint line almost midway between the  $Q(1)$  doublet of  $\lambda 5610$ ,  $\pi$  polarization.) In  $\lambda 5610$ , parallel ( $\pi$ ) and perpendicular ( $\sigma$ ) polarizations superposed, the triplets given by  $Q(1)$  and  $P(1)$  are to be noted. The  $Q(1)$  triplet is quite symmetrical in intensity with the central component, as shown by photometric curves just obtained, slightly stronger than the other components. The left component of the  $P(1)$  triplet, however, is so faint as to be scarcely recognizable on the reproduction (see Fig. 1). In the parallel polarization  $P(1)$  appears as a sharp singlet and  $P(2)$  as a triplet (with only two lines showing in the reproduction). The  $Q$  lines appear as doublets,  $Q(1)$  being a real doublet, the higher ones appearing as such due to the resolving power being much too low to reveal the fine structure. In second order plates this doublet appearance of the  $Q$  lines could be observed as far as  $Q(14)$ .  $\Delta\nu_n$  for  $H=24,000$  gauss is of the order of 1.1 wave number units.

*Other P lines.* The  $P(2)$  patterns were resolved in only two cases. In parallel polarization ( $\lambda 5610$ ) a very narrow and faint triplet was found of width 95 percent of that from Eq. (4A). In  $\lambda 5198$  in perpendicular polarization two very faint lines occur, one on either side of the strong line  $P(7)$ . They are of about equal intensity and perceptibly weaker than  $\sigma - Q(1)_0$ . The qualitative data on these  $P$  lines are summarized briefly in Table I. Under the caption "plates used" is given the number of plates from which the nature of a given pattern was determined. Cases rendered doubtful by reason of extreme faintness are marked with a question mark.

TABLE I

*P line patterns.*

Bracketed patterns indicate that part of pattern is obscured by some other line but that the part visible has proper position and magnitude. (See Fig. 4) Question marks indicate doubt due to great faintness or possible presence of impurities.

Polarization	Line	$\lambda 5610$			$\lambda 5198$			$\lambda 5835$			
		Nature	Remarks on intensity	Plates used	Nature	Remarks on intensity	Plates used	Nature	Remarks on intensity	Plates used	
$\pi$	$P(1)$	sharp singlet	same as $\pi - Q(1)_{+1}$	2	Doublet $< \pi - Q(1)_0$	1	sharp singlet	$> \pi - Q(1)_{-1}$	1		
$\sigma$	$P(1)$	triplet	Center component strongest and of intensity $> Q(1)_{\pm}$	2			[quartet] $\sigma - P(2)_{\pm 2}$ $< \sigma - Q(1)_0$	1	[Doublet]	?	1
$\pi, \sigma$	$P(1)$								[triplet]	central component most intense	1
$\pi$	$P(2)$	very narrow triplet	??	1							
$\sigma$	$P(2)$										

\*  $\pi - P(2)_{-1}$  seems to be anomalously faint and does not show in the reproduction in Fig. 5.

The patterns of the higher  $P$  lines, which are observable, are in parallel polarization all narrower than in perpendicular. In parallel polarization the intensity in a given pattern (unresolved in detail) is greatest in the center, while in the perpendicular polarization a distinct doublet effect is noticeable (less marked than for  $Q$  doublets). In the only case where the width of a  $P$  doublet could be measured with any precision a value agreeing closely with that for the corresponding  $Q$  doublet was obtained (see below).

*Q lines.* In the case of the  $Q$  lines the data are more complete as well as more certain. In parallel polarization  $Q(1)$  shows itself a doublet in all three bands. In the perpendicular polarization in  $\lambda 5610$  only  $\pi - Q(1)_0$  is visible and it is very faint (this doubtless accounts for the absence of the other components whose intensity from Fig. 1 should be only half as great). In  $\lambda 5198$  likewise only  $\pi - Q(1)_0$  is visible, the others here being obscured by  $\pi - Q(2)_{+2}$  and  $P_{10}$ .

On only two plates (see Table II) were  $Q(2)$  patterns resolved. The first, in  $\lambda 5610$ , due to the presence of  $P(9)$  shows only the right half of the pattern, and the second (due to nearness of  $\pi - Q(1)_{-1}$ ) gives only three of the four lines. In both cases, however, the outer components are three or four times as intense as the inner. While very difficult to measure with any



precision, the magnitudes of the separations average within 10 percent of the calculated ones.

TABLE II

*Q line patterns.*

Polarization	Line	$\lambda 5610$			$\lambda 5198$			$\lambda 4835$		
		Nature	Remarks on intensity	Plates used	Nature	Remarks on intensity	Plates used	Nature	Remarks on intensity	Plates used
$\pi$	Q(1)	doublet	$\pi-Q(1)_{+1}$ more intense than $\pi-Q(1)_{-1}$ very faint	1	[doublet]		2	[doublet]	very faint	1
$\sigma$	Q(1)	single†		1	[triplet]	Central component only visible*	1			
$\pi, \sigma$	Q(1)	triplet	Q(1) <sub>0</sub> fainter than Q(1) <sub>±1</sub>	2	[triplet]		1	[triplet]	very faint	1
$\pi$	Q(2)	quartet	$\pi-Q(2)_{-1}$ very faint	1	[quartet]	$\pi-Q(2)_{±}$ much fainter than $\pi-Q(2)_{-2}$				

\* This component is more intense than  $\pi-P(1)_{+1}$  or  $\pi-P(1)_{-1}$ . (See Table I).

† Should be triplet. (Outer components probably too faint to show. See Fig. 1).

The patterns for the higher  $Q$  lines are in rather striking harmony with the theory. In perpendicular polarization they are simply broadened to approximately the same width as corresponding  $R$  lines. With both polarizations superposed a distinct lightness in the center is observable (in all three bands) up to  $Q(4)$  or  $Q(5)$ , beyond which the pattern is too narrow for observation of the effect. In the parallel polarization the  $Q$  lines appear as distinct doublets, the centers being very much lighter and the doublet components much sharper than in the case of the corresponding  $P$  and  $R$  doublets. (see Fig. 5) It was found possible to measure these doublet widths (by use of both first and second-order plates) up to  $Q(14)$  for  $\lambda 5610$ , to  $Q(8)$  for  $\lambda 5198$  and to  $Q(7)$  for  $\lambda 4835$ . These results expressed as percentages of  $\Delta\nu_n$  and averaged for the two available plates of each band are represented in Fig. 6.<sup>30</sup> (Since the fields differed on the two plates by only 150 gauss, this averaging is quite justified even though the rigid proportionality of the separation to field strength has been only approximately established.

The observed doublets, at least those with  $M > 2$ , evidently represent two unresolved groups of lines corresponding to the outer and more intense parts of the theoretical patterns. Fig. 1 in fact shows that in measuring the doublets, since settings are made on the apparent centers of gravity of the two doublet members, the observed widths will of necessity be less than the theoretical maximum pattern widths. This is amply borne out by the data given in Table III and plotted in Fig. 6. The two smooth curves are calculated from Eqs. (6) and (7), the ordinates representing percentages of  $\Delta\nu_n$ . The two curves for all values of  $M$  greater than unity are so nearly coincident that the present data could not be expected to favor one more than the other.

<sup>30</sup> The difficulty in measurement of the doublets is due to the low intensity of the patterns for small  $M$  values and the lack of definition of those for large  $M$  values. Each value represents the average of from 20–30 measurements.

The most trustworthy value for total pattern width of lines with  $M=1$  is 94.8 percent of  $\Delta\nu_n$ , the five other values obtained agreeing with this to within less than 2 percent. Consequently all the observed points lie midway between the two theoretical curves. The best results for  $M=2$  are not of comparable accuracy, but give for the pattern width 63 percent of  $\Delta\nu_n$  (i.e. 99 and 94 percent of the values predicted, respectively, by Eqs. (3A) and (4A)). The results for the patterns of higher  $M$  values being taken from the  $Q$  doublets (parallel polarization) must, as explained above, fall a certain amount below the theoretical predictions. As a matter of fact for  $\lambda\lambda 5610$  and  $5198$  between  $Q(3)$  and  $Q(14)$  the observed doublet widths average

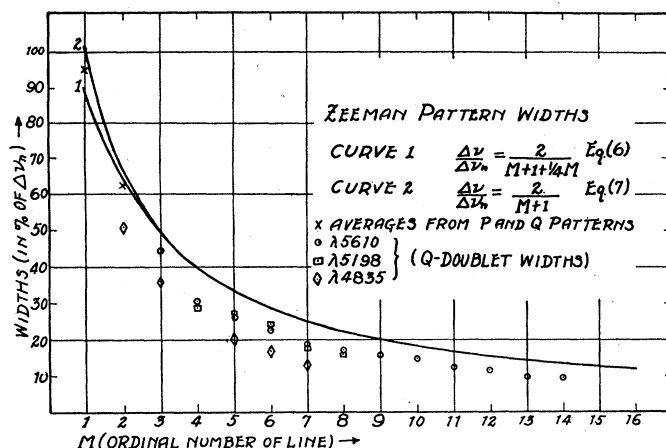


FIG. 6. The widths of resolved patterns having  $M$ -values 1 and 2, i.e. those of  $P(1)$ ,  $Q(1)$ ,  $P(2)$ ,  $Q(2)$ , are averaged and plotted as  $x$ . The other points represent widths of  $Q$  doublets and fall regularly below the theoretical extreme widths for reasons given under Table III. The  $M$ -values used as abscissas are the empirical ordinal numbers of the lines in their respective bands. They are numerically equal to the final  $j$ -values of the new, and  $\frac{1}{2}$  unit smaller than the final  $j$ -values of the old quantum theory.

77 percent of the theoretical total widths. Why the values from  $\lambda 4835$  should fall below the rest as they do is not clear.<sup>31</sup>

*R lines.* The  $R$  lines were so weak on all of the plates that no  $R$  pattern was definitely resolved. The higher  $R$  lines behave quite similarly to the  $P$  lines except that they have the same widths in both polarizations and the lightness in the center (perpendicular polarization) is much less marked than for  $P$  lines of the same  $M$  value. This doublet-character was visible for  $R(3)$ ,  $R(4)$  and  $R(5)$  in  $\lambda 5610$  and  $R(4)$  in  $\lambda 4835$  (not observable in  $\lambda 5198$ ; see Fig. 4). With both polarizations superposed the results were qualitatively the same as for parallel polarization except that  $R(2)$  here seemed to have a

<sup>31</sup> For a further check the over-all widths (measured from edge to edge) of the  $Q$  patterns taken with both polarizations superposed were measured. These magnitudes although not very precisely defined, all fall regularly above the theoretical curves of Fig. 6.

light streak in the center. This shows on only one plate of one band<sup>32</sup> and if confirmed represents a distinct disagreement with the theoretical expectations.

TABLE III

*P and Q doublet separations.* The values given in this table are expressed as percentages of  $\Delta\nu_n$  the normal Lorentz separation. Those for  $P(1)$ ,  $P(2)$ ,  $Q(1)$ , and  $Q(2)$  of  $\lambda\lambda 5610$  and  $5198$  are total widths of resolved patterns, that for  $Q(1)$  in  $\lambda 5610$  being the most reliable. The other values represent  $Q$  doublet separations in parallel polarization. Since we are for these measuring not the distance between sharp lines, but the distance between the centers of gravity of unresolved patterns, Fig. 1 predicts that such measurements must give values which are less than the theoretical separations of the outermost components. These latter theoretical separations as calculated from Eqs. (6) and (7) are given at the bottom of the table

Band	Line	$P(1)$	$P(2)$	$P(6)$	$Q(1)$	$Q(2)$	$Q(3)$	$Q(4)$	$Q(5)$	$Q(6)$	$Q(7)$	$Q(8)$	$Q(9)$	$Q(10)$	$Q(11)$	$Q(12)$	$Q(13)$	$Q(14)$
$\lambda 5619$	width	96.1		21	94.8	60*	44.5	30.4	26.1	22.8	18.9	17.0	15.3	14.8	12.3	11.8	9.7	9.5
	No. of plates	1		1	1	1	2	2	2	2	2	2	1	1	1	1	1	1
$\lambda 5198$	width	93	62		94.2	65		28.7	27.4	24.3	18.0	16.0						
	plates	1	1		2	1		2	2	3	3	1						
$\lambda 4835$	width					51	35.7		20	16.8	13							
	plates					2	2		1	1	1							
Eq. (6)	width	100.0	66.7	28.6	100.0	66.7	50.0	40.0	33.3	28.6	25.0	22.2	20.0	18.2	16.7	15.4	14.3	13.3
	width	88.9	64.0	28.4	88.9	64.0	49.0	39.5	33.0	28.4	24.9	22.1	20.0	18.2	16.7	15.4	14.3	13.3

\* Calculated from displaced position of line.

*Conclusions.* Summing up, then, we find that eight of the twelve patterns given in Fig. 1 as characteristic for the first two lines of the  $P$  and  $Q$  branches have been resolved. The corresponding  $R$  lines were too faint for observation. The unresolved patterns of the higher lines of all three branches in the various polarizations behave in the definite and characteristic way predicted by theory. The results definitely confirm the classification of the Angstrom CO bands as  $^1S \rightarrow ^1P$  with  $\sigma' = 0$ ,  $\sigma'' = 1^6$ .

The intensity relations among the components of the resolved patterns have in the main supported the summation rule predictions, at least as far as correct order of intensities is concerned (visual estimates.)<sup>33</sup> Departures from the theoretical intensity relations are of three sorts, of which the first two, occurring on one plate only, are doubtful, while the last, being found in the case of about fifteen lines in four different bands is definitely established. The doubtful conflicts with theory are: the somewhat greater intensity of  $\sigma - \pi - P(1)_{-1}$  as compared with  $\sigma - \pi - P(1)_{+1}$  (i.e. the greater intensity of the high-frequency component); and the occurrence in the case of the  $R(2)$  pattern (on the same plate) of a slight but distinct lightness in the center (see Fig. 1). The definite and well-supported departure from theory is the occurrence of distinctly greater intensity in the low frequency than in the high-frequency members of  $Q$  doublets as observed in parallel polarization, the dissymmetry gradually decreasing for higher  $M$  values ceasing to be observable beyond  $M = 6$ . Since in the case of the  $Q(1)$  pattern with

<sup>32</sup> This is the *only* plate on which  $R(2)$  shows distinctly enough for observation.

<sup>33</sup> Dr. O. Sandvik of the Eastman Kodak Research Laboratories has kindly made microphotometric curves of some of our better plates. The results which it is hoped to give in another paper are in accord with the above, particularly as to the predicted fact that  $\pi - \sigma - Q(1)_0$  should be slightly less intense than  $\pi - \sigma - Q(1)_{+1}$  or  $\pi - \sigma - Q(1)_{-1}$ .

both polarizations superposed this dissymmetry has disappeared, it must follow that the reverse order of intensity must hold for the outer components in the perpendicular polarization alone.<sup>34</sup>

The magnitudes of the patterns are directly proportional to the field strengths. The widths of the  $P(1)$  and  $Q(1)$  patterns average 95 percent of  $\Delta\nu_n$  and thus fall midway between the 88.9 and 100 percent of  $\Delta\nu_n$  predicted respectively by Eqs. (6) and (7) for  $M=1$ . The patterns of the other lines are of the expected magnitude, the  $Q$  doublets in particular falling regularly (as anticipated for reasons already given) somewhat below the theoretical curves for maximum pattern widths.

Since, according to theory, the nature of the Zeeman effect varies with the type of electronic transitions involved, it should give valuable information as to what sort of transitions give rise to a given set of bands, the characteristic behavior of the various branches further enabling the quantum analysis of a given band to be carried through more readily than otherwise.

We are under great obligation to the Milton Fund of Harvard University for a generous grant which made our experimental work possible.

JEFFERSON PHYSICAL LABORATORY,  
HARVARD UNIVERSITY,  
July, 1927.

<sup>34</sup> This could not be determined directly from the plates thus far obtained.

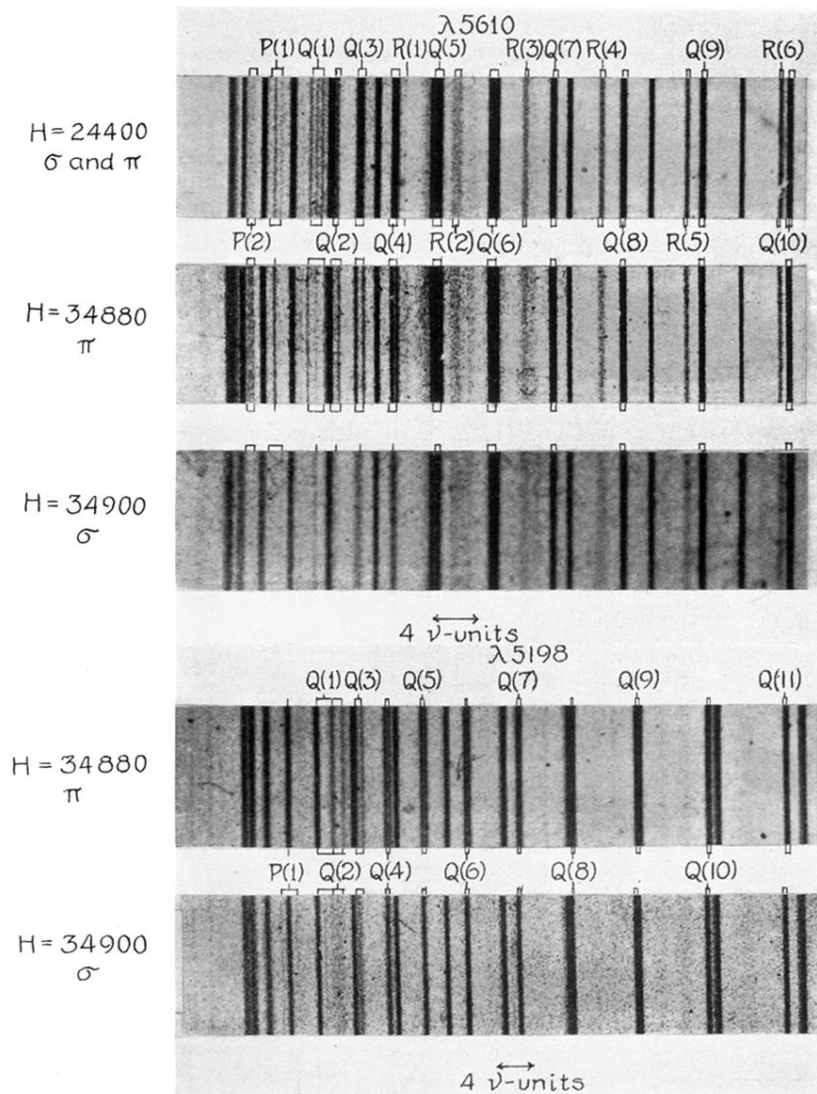


Fig. 5. These reproductions represent enlargements (about 15 times) of regions near the heads of the  $\lambda\lambda 5610$  and  $5198$  bands. In order to insure the reproduction of at least some of the fainter patterns the left ends of the bands (as explained in the text) were exposed longer in printing than the rest. Consequently the patterns of the  $P(1)$ ,  $P(2)$ ,  $Q(1)$ , and  $Q(2)$  lines have a much greater relative intensity than on the original plates. Faint lines not marked are impurities (including the faint line almost midway between the  $Q(1)$  doublet of  $\lambda 5610$ ,  $\pi$  polarization.) In  $\lambda 5610$ , parallel ( $\pi$ ) and perpendicular ( $\sigma$ ) polarizations superposed, the triplets given by  $Q(1)$  and  $P(1)$  are to be noted. The  $Q(1)$  triplet is quite symmetrical in intensity with the central component, as shown by photometric curves just obtained, slightly stronger than the other components. The left component of the  $P(1)$  triplet, however, is so faint as to be scarcely recognizable on the reproduction (see Fig. 1). In the parallel polarization  $P(1)$  appears as a sharp singlet and  $P(2)$  as a triplet (with only two lines showing in the reproduction). The  $Q$  lines appear as doublets,  $Q(1)$  being a real doublet, the higher ones appearing as such due to the resolving power being much too low to reveal the fine structure. In second order plates this doublet appearance of the  $Q$  lines could be observed as far as  $Q(14)$ .  $\Delta\nu_n$  for  $H=24,000$  gauss is of the order of 1.1 wave number units.